

# p37 Is a p97 Adaptor Required for Golgi and ER Biogenesis in Interphase and at the End of Mitosis

Keiji Uchiyama,<sup>1,7</sup> Go Totsukawa,<sup>1,7</sup> Maija Puhka,<sup>2,7</sup> Yayoi Kaneko,<sup>1</sup> Eija Jokitalo,<sup>2</sup> Ingrid Dreveny,<sup>3</sup> Fabienne Beuron,<sup>3</sup> Xiaodong Zhang,<sup>3</sup> Paul Freemont,<sup>3</sup> and Hisao Kondo<sup>1,4,5,6,\*</sup>

<sup>1</sup> Mitsubishi Kagaku Institute of Life Sciences  
Tokyo 194-8511

Japan  
<sup>2</sup> Institute of Biotechnology  
University of Helsinki  
Helsinki FIN-00014

Finland  
<sup>3</sup> Centre for Structural Biology  
Imperial College London  
London SW7 2AZ  
United Kingdom

<sup>4</sup> Graduate School of Medical Science  
Kyushu University  
Fukuoka 812-8582

Japan  
<sup>5</sup> Cambridge Institute for Medical Research  
University of Cambridge  
Cambridge CB2 2XY  
United Kingdom

<sup>6</sup> SORST  
Japan Science and Technology Agency  
Saitama 332-0012  
Japan

## Summary

We previously reported that p97/p47-assisted membrane fusion is important for the reassembly of organelles at the end of mitosis, but not for their maintenance during interphase. We have now identified a p97 adaptor protein, p37, which forms a complex with p97 in the cytosol and localizes to the Golgi and ER. siRNA experiments revealed that p37 is required for Golgi and ER biogenesis. Injection of anti-p37 antibodies into cells at different cell cycle stages showed that p37 plays an important role in both Golgi and ER maintenance during interphase as well as in their reassembly at the end of mitosis. In an *in vitro* Golgi reassembly assay, the p97/p37 complex has membrane fusion activity. In contrast to the p97/p47 pathway, this pathway requires p115-GM130 tethering and SNARE GS15, but not syntaxin5. Interestingly, although VCIP135 is also required, its deubiquitinating activity is unnecessary for p97/p37-mediated activities.

## Introduction

The Golgi apparatus occupies a central position in the secretory pathway, where it receives the entire output of *de novo*-synthesized proteins from the ER, and functions to distil, posttranslationally process, and sort

cargo to their ultimate destinations. The Golgi is fragmented into many small vesicles and short tubules during mitosis and is rapidly reassembled from such fragments within each daughter cell (Luocq *et al.*, 1989). Experiments conducted with an *in vitro* function assay, which mimics Golgi reassembly at the end of mitosis, showed that reassembly from membrane fragments requires at least two ATPases: N-ethylmaleimide-sensitive factor (NSF) and p97 (also known as VCP) (Rabouille *et al.*, 1995a). The role of NSF has been well characterized, while much less is known about the mechanism of action of p97. Two cofactors have so far been identified, namely, p47 and VCIP135 (VCP[p97]/p47 complex-interacting protein, p135). p47 forms a tight complex with p97, which is essential for *in vitro* Golgi reassembly (Kondo *et al.*, 1997). The SNARE protein (soluble NSF attachment protein [SNAP] receptor) syntaxin5 is a receptor in Golgi membranes for the p97/p47 complex, and p47 mediates the binding of p97 to syntaxin5 (Rabouille *et al.*, 1998). VCIP135 binds to the p97/p47/SNARE complex and dissociates it via p97-catalyzed ATP hydrolysis (Uchiyama *et al.*, 2002). Recently, VCIP135 has been reported to possess deubiquitinating activity (Wang *et al.*, 2004).

We previously showed that the injection of anti-p47 antibodies into mitotic cells inhibited the reassembly of Golgi and ER in daughter cells (Uchiyama *et al.*, 2002). We also reported that mitotic phosphorylation of p47 is important for Golgi disassembly at the onset of mitosis, as microinjection of p47(S140A), which is unable to be phosphorylated, allows cells to maintain Golgi stacks during mitosis. Consequently, the membrane fusion activity assisted by the p97/p47 complex is thought to be important for the reassembly of organelles at the end of mitosis (Uchiyama *et al.*, 2003). However, p47 has two nuclear localization signals and mainly localizes to the nucleus in interphase cells. The injection of highly concentrated anti-p47 antibodies into the cytoplasm of interphase cells does not result in any morphological changes. It is therefore likely that p97/p47-assisted membrane fusion is less critical during interphase than at the end of mitosis (Uchiyama *et al.*, 2003). These observations pose the question: Does p97 have another pathway besides the p97/p47 pathway for the maintenance of organelles during interphase? Alternatively, is p97-assisted membrane fusion not necessary for the maintenance of organelles in interphase cells? Dalal *et al.* (2004) indeed reported that no morphological change was observed in Golgi when a p97 mutant lacking ATPase activity was expressed in culture cells. However, it is possible that the inactivation of the endogenous p97 might be insufficient to inhibit p97-assisted membrane fusion in their study.

Here, we report a novel membrane fusion pathway that requires the p97/p37 complex. p37 forms a tight complex with p97 in the cytosol. This adaptor protein of p97 localizes to the Golgi and ER and is required for their maintenance during interphase as well as for their reassembly at the end of mitosis. The p97/p37 complex also shows membrane fusion activity in an *in vitro* Golgi

\*Correspondence: [hk228@molbiol.med.kyushu-u.ac.jp](mailto:hk228@molbiol.med.kyushu-u.ac.jp)

<sup>7</sup> These authors contributed equally to this work.

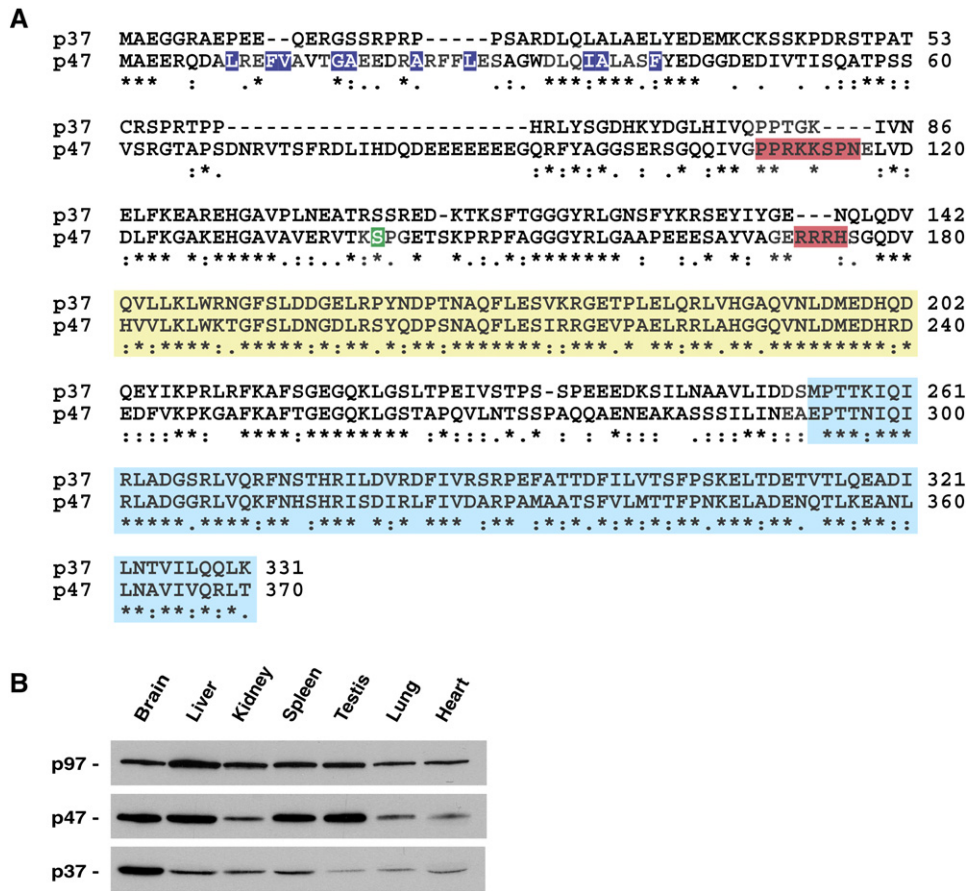


**Figure 1.** p37 Is Similar to p47  
(A) Amino acid sequence alignment of p37 and p47. The C-terminal p47 UBX domain (shaded in light blue) is highly homologous to the predicted p37 UBX domain (~63% sequence identity). The SEP domain (shaded in yellow) is also found in p37 (~72% sequence identity). The p47 phosphorylation site at serine-140 is shaded in green, and the two p47 nuclear localization signals missing in p37 are shaded in red. p37 does not contain a defined N-terminal UBA domain; hydrophobic core residues in the p47 UBA domain (shaded in blue) are not well conserved, and some residues are missing. Identical residues between the two proteins are marked with asterisks.  
(B) The amount of p37 in various tissues. Rat tissue proteins were extracted from 0.2 mg (wet weight) of tissue in sample buffer and fractionated by SDS-PAGE. Blots were probed with polyclonal antibodies to p97, p47, and p37.

reassembly assay; however, this activity has several important mechanistic differences compared to that of p97/p47-assisted membrane fusion.

**Results**

**p37 Forms a Complex with p97**

Since p47 mainly localizes to the nucleus at interphase, p97/p47-assisted membrane fusion is not critical for the maintenance of Golgi during interphase (Uchiyama et al., 2003). In contrast to the subcellular distribution of p47, p97 localizes to both the nucleus and the cytoplasm at interphase. Hence, it is plausible that p97 may have another adaptor, which localizes to the cytoplasm during interphase, for the maintenance of Golgi and ER.

Furthermore, the expression of such a cofactor might be expected to be higher in nonproliferating tissues, such as brain, than in proliferating tissues. We therefore used a brain cDNA library to perform a yeast two-hybrid screen, and we identified one clone that had a predicted peptide sequence similar to that of p47; its predicted

molecular weight was 37 kDa, and, hence, we called it “p37” (Figure 1A). The UBX and SEP domains, which are important for p47 binding to p97, are highly homologous between p37 and p47. Interestingly, the two nuclear localization signals present in p47 are absent in p37. p37 doesn’t contain a defined UBA domain, which is important for the binding to ubiquitin; key hydrophobic core residues in the p47 UBA domain (Figure 1A, shaded in blue) are not well conserved in p37, and some residues are missing.

As shown in Figure 1B, western blotting confirmed the existence of p37 in brain, liver, kidney, spleen, testis, lung, and heart. p37 was present in all tissues studied and was especially abundant in brain.

Since p37 has both the UBX and SEP domains, we would expect p37 to bind to p97. We tested this by using several biochemical techniques. Figure 2A shows the results of coimmunoprecipitation from rat brain cytosol. Anti-p37 antibodies pulled down a protein of 97 kDa (left), which was shown to be p97 by western blotting (right top). However, p47 could not be detected in the precipitates (right middle). These data suggest that

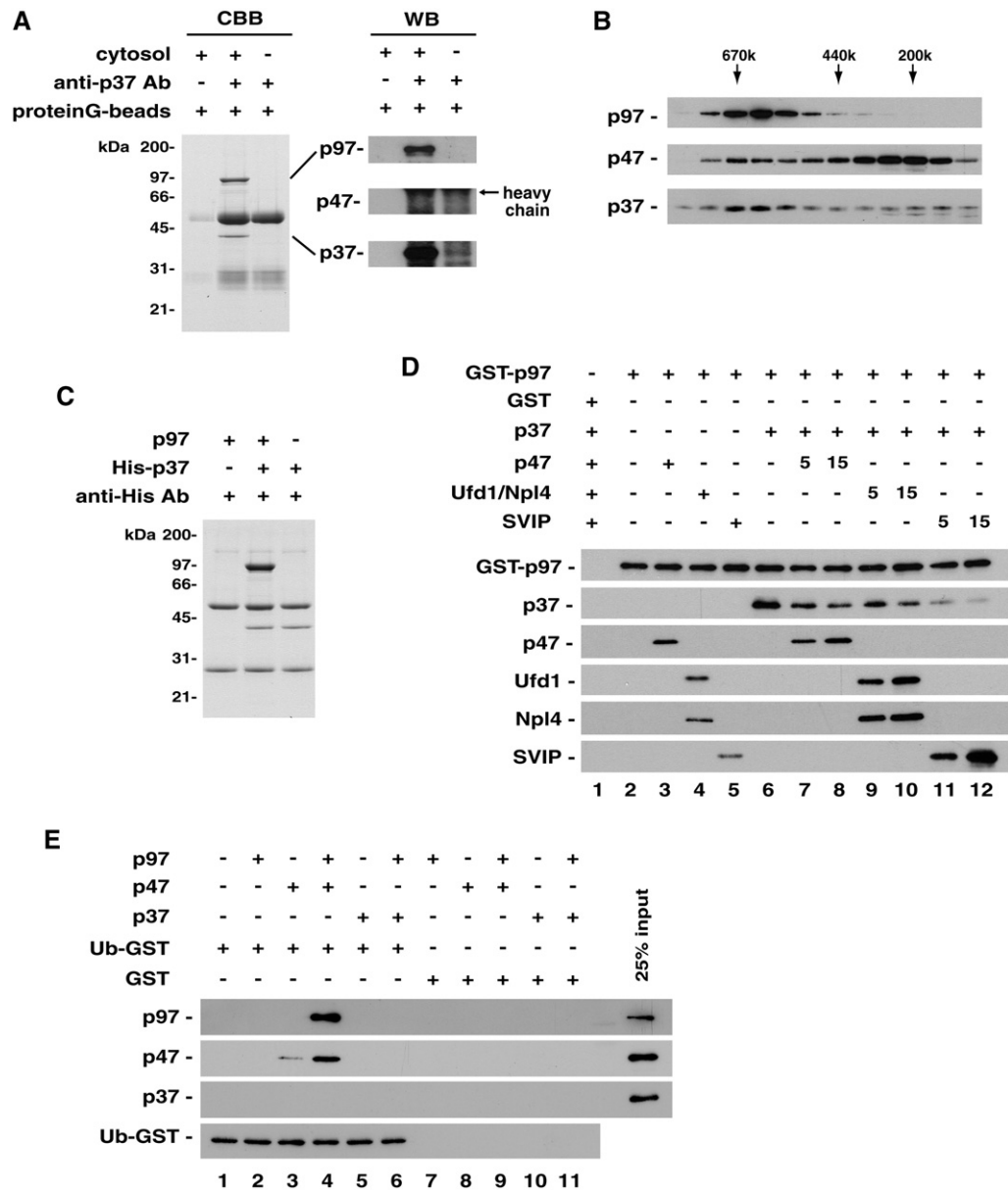


Figure 2. p37 Forms a Complex with p97

(A) Rat brain cytosol was incubated with anti-p37 antibodies. The immunoprecipitates were fractionated by SDS-PAGE, followed by staining with Coomassie blue (CBB, left panel) and western blotting with antibodies to p97, p47, and p37 (WB, right panels).  
 (B) Rat brain cytosol was size fractionated by gel filtration, and the fractions were assayed by western blotting.  
 (C) His-tagged p37 was incubated with an excess amount of p97 in a buffer containing 0.15 M KCl and 0.1% Triton X-100 on ice, then precipitated by anti-His tag antibodies. p37 and bound p97 were separated by SDS-PAGE and stained with CBB.  
 (D) GST-tagged p97 (0.3  $\mu$ g) was incubated with the indicated His-tagged proteins (p37, 0.3  $\mu$ g; p47, 0.4, 2, or 6  $\mu$ g; Ufd1, 0.3, 1.5, or 4.5  $\mu$ g; Npl4, 0.6, 3, or 9  $\mu$ g; SVIP, 0.15, 0.75, or 2.25  $\mu$ g) in a buffer containing 0.15 M KCl, 0.1% Triton X-100, and 5 g/l trypsin inhibitor on ice, then isolated on glutathione beads; bound proteins were fractionated by SDS-PAGE. The blots were probed with antibodies to p97 and His tag.  
 (E) GST-tagged ubiquitin (Ub-GST, 0.4  $\mu$ g) was incubated with the indicated proteins (p97, 0.1  $\mu$ g; p47, 0.05  $\mu$ g; p37, 0.05  $\mu$ g), then isolated on glutathione beads; bound proteins fractionated by SDS-PAGE. The blots were probed with antibodies to p97, p47, p37, and Ub.

p37 can form a stable complex with p97 in the cytosol, and that p47 is not part of this complex. As presented in Figure 2B, fractionation of the cytosol by gel filtration showed that p37 mainly distributed to the p97-containing fractions. These results strongly indicate that p37 exists mainly in the form of a p97/p37 complex in the cytosol. We next performed binding experiments with purified recombinant proteins. An excess amount of p97

was incubated with His-tagged p37. p37 and bound p97 were immunoprecipitated with anti-His antibodies and were separated by SDS-PAGE, followed by CBB staining (Figure 2C). p37 and p97 clearly formed a complex, and the ratio of p97 to p37 was estimated as 2:1 (mol:mol) from the densities of the bands.

The next question was whether this p97/p37 complex is distinct from known p97-containing complexes. To

address this, we carried out competition experiments, which are shown in [Figure 2D](#). p37 and GST-tagged p97 were incubated in the absence or presence of the known p97 adaptors: p47, Ufd1/Npl4, and SVIP ([Kondo et al., 1997](#); [Meyer et al., 2000](#); [Nagahama et al., 2003](#)). We found that p47, Ufd1/Npl4, and SVIP all inhibited the binding of p37 to p97 (p47, lanes 7–8; Ufd1/Npl4, lanes 9–10; SVIP, lanes 11–12), indicating that p37 is not a constituent of the p97/p47, p97/Ufd1/Npl4, or p97/SVIP complexes. Given that we observed no bands other than p97 and p37 in the coimmunoprecipitation experiments ([Figure 2A](#), left), we concluded that p37 forms a novel, to our knowledge, stable complex with p97.

p47 has a UBA domain and is reported to bind to ubiquitin in the presence of p97 ([Meyer et al., 2002](#)). In contrast, protein structure analysis including fold recognition predicts that p37 does not contain a defined UBA domain ([Figure 1A](#)), suggesting that p37 does not bind ubiquitin. To confirm this, we investigated ubiquitin binding to p37 ([Figure 2E](#)). For comparison, p47 bound ubiquitin in the presence of p97 (lane 4), while p37 did not bind ubiquitin in either the presence or absence of p97 (lanes 5–6) under the same experimental conditions.

### p37 Is Important for the Biogenesis of the Golgi and ER In Vivo

The subcellular distribution of p37 was determined by immunofluorescence microscopy with PFA fixation. p37 existed both in the cytoplasm and nucleus ([Figure 3A](#), left), whereas p47 mainly localized to the nucleus (middle). This is consistent with the lack of a defined nuclear localization signal motif in p37 ([Figure 1A](#)). We next clarified the localization of membrane-bound p37 by using methanol fixation. As shown in [Figures 3B](#) and [3C](#), double immunofluorescence staining of p37 with either GM130, a Golgi marker, or protein disulfide isomerase (PDI), an ER marker, showed the localization of p37 to both the Golgi and ER. Given the similarity of p37 to p47 ([Figure 1A](#)), we wanted to test whether p37, like p47, plays a role in the biogenesis of the Golgi and ER ([Uchiyama et al., 2002](#)).

We first carried out p37-knockdown experiments by using siRNA ([Figures 4A–4C](#)). Two distinct p37 siRNA duplexes, specific for the nucleotide sequence of human p37, were used in HeLa cells. In p37 siRNA-treated cells, p37 was undetectable by immunofluorescence staining ([Figure 4A](#), [e] and [f]). Western blotting also showed that both p37 siRNA duplexes decreased p37 levels to <5% of its original level ([Figure S1A](#); see the [Supplemental Data](#) available with this article online). In p37-depleted cells, the Golgi still localized to a perinuclear region ([Figure 4A](#), [b] and [c]). The ultrastructures of the Golgi apparatus were further investigated by electron microscopy ([Figures 4B](#) and [4C](#)). In p37-depleted cells, the typical big stacks of Golgi were rarely observed, and large-scale vesiculation was present ([Figure 4B](#), top right and bottom panels). Membrane profiles in the Golgi area were calculated, and the results are shown in [Figure 4C](#). Both p37 siRNAs significantly decreased the percentage of membranes in Golgi cisternae, while they increased the percentage of tubules and vesicles within the Golgi area, compared with mock control. These results strongly suggest that p37 is important for the biogenesis of Golgi.

We have shown that p37 exists in the cytoplasm during interphase ([Figure 3](#)), but does p37 function in the maintenance of Golgi during interphase? To study this, we injected anti-p37 antibodies into the cytoplasm of interphase cells and investigated the ultrastructures of their Golgi by electron microscopy. The cells that had passed through mitosis were excluded in order to study only interphase cells. [Figure 4D](#) shows the quantitative results. The injection of anti-p37 antibodies significantly decreased the percentage of membranes in Golgi cisternae, and it significantly increased the percentage of tubules and vesicles, compared with the injection of random IgG (control). These effects were not observed when quenched antibodies were injected. Next, we injected the same antibodies into mitotic cells and investigated the effects on Golgi reassembly at the end of mitosis. Cells at prophase (or early prometaphase) were injected with anti-p37 antibodies and were fixed after they entered interphase. The injection of the antibodies had no effect on cell cycle progression. As shown in [Figure 4E](#), in antibody-injected daughter cells, the percentage of cisternae significantly decreased in the Golgi area, although this decrease was smaller compared with that observed for injected interphase cells. The percentage of tubules in the Golgi area was significantly increased by the injection of anti-p37 antibodies. These results strongly suggest that p37 plays an important role in Golgi maintenance during interphase as well as in its reassembly at the end of mitosis.

We next investigated the role of p37 on the biogenesis of ER. [Figure 5A](#) shows ER structures in mock- and p37 siRNA-treated cells. Two distinct p37 siRNA duplexes suppressed the p37 level to <5% of its original level ([Figure S1B](#)). Both p37 siRNA duplexes caused the formation of a large, meshed ER network (the middle and right panels of [Figure 5A](#)), which was not observed in mock-treated cells (the left panel in [Figure 5A](#)). To quantify the degree of ER network formation, the number of three-way junctions was counted in living cells by using confocal microscopy, and the results are presented in [Figure 5B](#). The number of three-way junctions was significantly decreased by p37 siRNA treatments. We also injected anti-p37 antibodies into cells at different cell cycle stages. As presented in [Figures 5C](#) and [5D](#), the injection of anti-p37 antibodies into interphase and mitotic cells significantly decreased the number of ER three-way junctions to ~35% and ~60% of control (random IgG injection), respectively. These changes disappeared by quenching the antibodies. All of these results indicate that p37 functions in ER network formation.

The importance of p37 in the maintenance of the ER and Golgi suggests that p37 has possible functions in membrane trafficking from the ER to the plasma membrane. To test this, we depleted p37 in living cells and studied the transport of VSV-G, a reporter protein for membrane transport in secretory pathways. A thermoreversible folding mutant of VSV-G fused to GFP at its C terminus (ts045-VSV-G-GFP). This mutant misfolds and is retained in the ER at 39.5°C; however, upon a temperature shift to 32°C, it can fold and be transported to the Golgi and, subsequently, to the plasma membrane. The results are presented in [Figures 6A](#) and [6B](#). In mock-transfected cells, ts045-VSV-G-GFP was transported to the Golgi at the 20 min time point ([Figure 6A](#), upper

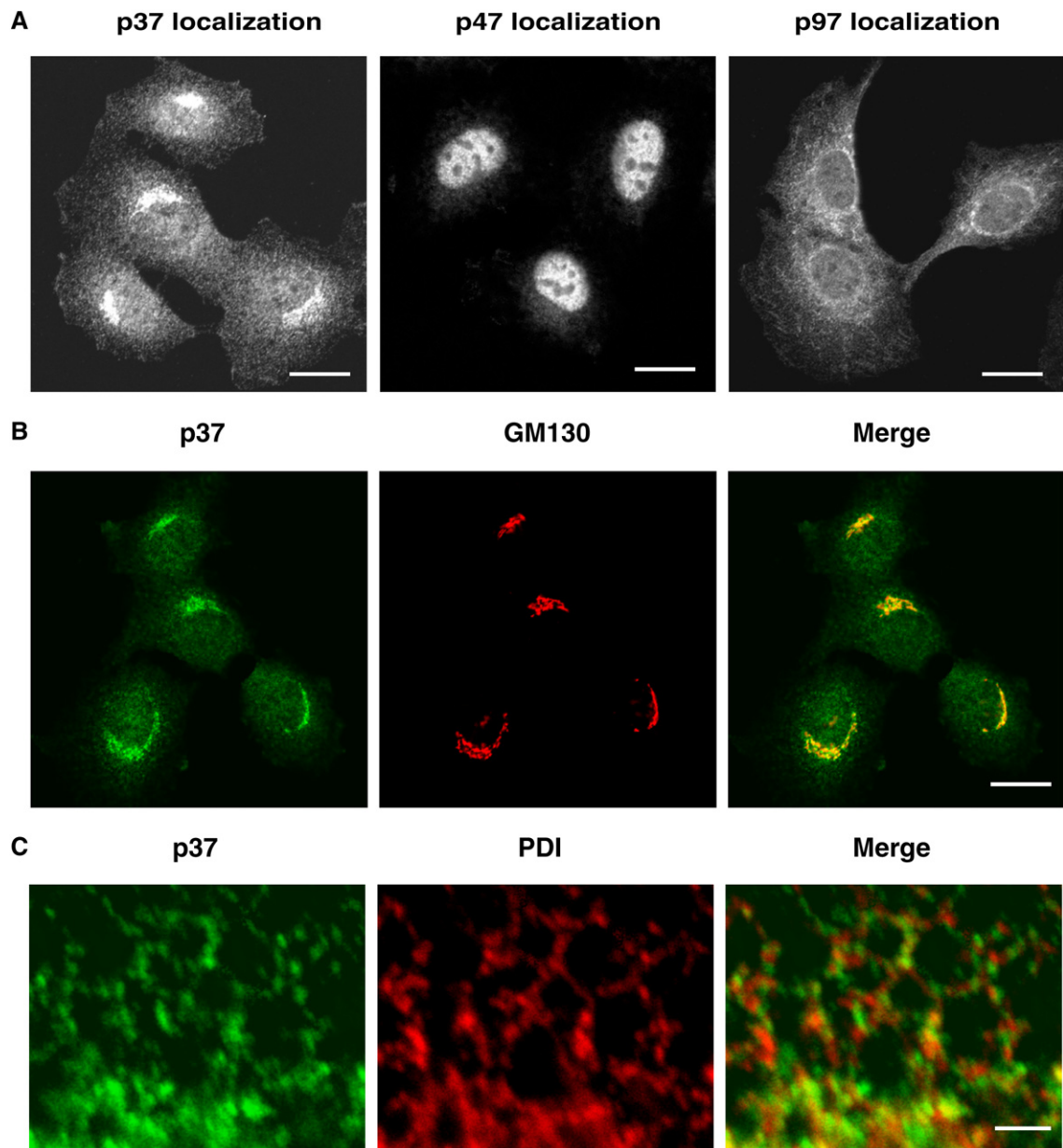


Figure 3. p37 Localizes to the Golgi and ER during Interphase

(A) The distribution of p37, p47, and p97. NRK cells were fixed with paraformaldehyde, permeabilized with Triton X-100, stained with polyclonal antibodies to p37, p47, and p97, and observed by confocal microscopy. The scale bar is 10  $\mu\text{m}$ .

(B) Double immunofluorescence staining of p37 and GM130, a Golgi marker, shows that p37 localizes to the Golgi. NRK cells were fixed with methanol at  $-20^{\circ}\text{C}$  for 4 min, stained with antibodies, and observed by confocal microscopy. The scale bar is 10  $\mu\text{m}$ .

(C) Double immunofluorescence staining of p37 and PDI, an ER marker, shows that p37 localizes to the ER. CHO cells were fixed with methanol at  $-20^{\circ}\text{C}$  for 4 min, stained with antibodies, and observed by confocal microscopy. The scale bar is 2  $\mu\text{m}$ .

middle) and to the plasma membrane at the 60 min time point (upper right). In p37-depleted cells, ts045-VSV-G-GFP was transported to the Golgi at the 20 min time point (lower middle) and still remained in the Golgi at the 60 min time point (lower right). To quantify these observations, more than 400 cells per time point were counted, and the calculated results are presented in [Figure 7B](#). In the p37-depleted cells, there was no change in the ER-to-Golgi transport of ts045-VSV-G-GFP, but its transport through the Golgi was delayed (right panel, red line). The delay might be explained by the disruption

of Golgi structures caused by p37 siRNA treatment. There still remain some possibilities that p37 may also play a role in the transport of vesicles from the Golgi to the plasma membrane.

Since p97 is reported to be involved in ER-associated degradation (ERAD) as well as in membrane fusion ([Ye et al., 2001](#)), we tested whether the depletion of p37 had some effects on ERAD. The turnover of a model ERAD substrate,  $\Delta\text{F508CFTR}$ , was investigated to estimate ERAD activity. As presented in [Figure 6C](#), there was no difference in  $\Delta\text{F508CFTR}$  turnover between

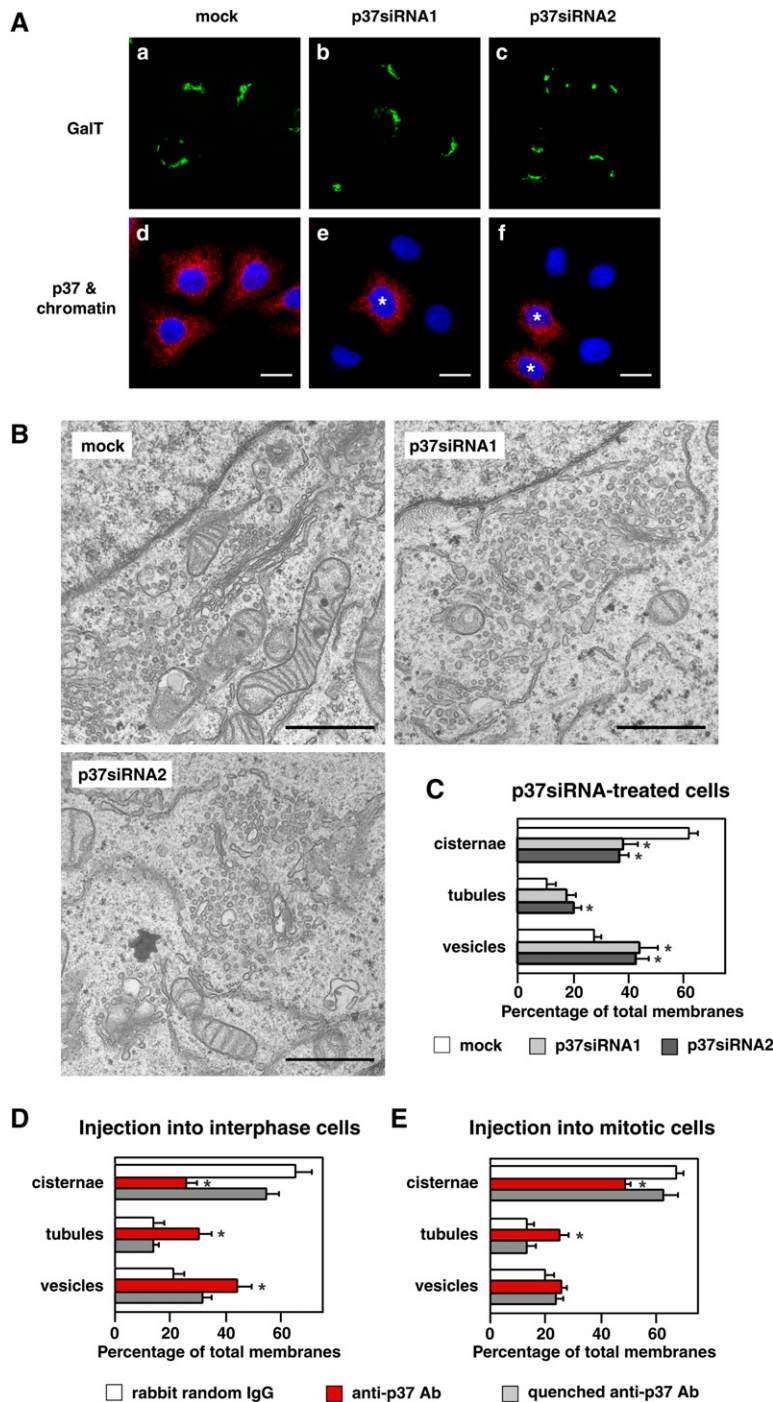


Figure 4. p37 Is Essential for the Biogenesis of the Golgi In Vivo

(A) HeLa cells were either mock transfected with water or transfected with two distinct siRNA duplexes specific to p37. The cells were incubated for 48 hr and then fixed. Since the transfection efficiency was ~90%, especially in these images, untransfected cells (asterisk [e] and [f]) were cocultured 24 hr after transfection in order to set a control. Golgi (green, [a]–[c]), p37 (red, [d]–[f]), and chromatin (blue, [d]–[f]) were stained by monoclonal anti-GalT antibodies, polyclonal anti-p37 antibodies, and DAPI, respectively. The scale bar is 10  $\mu$ m.

(B) Representative EM images of Golgi in either mock- or p37 siRNA-treated HeLa cells. The scale bar is 0.5  $\mu$ m.

(C) Golgi membranes in either mock- or p37 siRNA-treated HeLa cells were classified into cisternae, vesicles, and tubules and were counted as previously described (Shorter and Warren, 1999). Means  $\pm$  SD (n = 8). An asterisk indicates a significant difference at  $p < 0.05$  compared with mock (Bonferroni method).

(D) NRK cells at interphase were injected with anti-p37 antibodies, incubated for 4 hr, and then fixed. The cells that entered mitosis were removed every 1.5–2 hr during the incubation in order to confirm that the remaining cells had never passed through mitosis. Golgi membranes in injected cells were classified and counted. Means  $\pm$  SD (n = 7). An asterisk indicates a significant difference at  $p < 0.05$  compared with random IgG (control).

(E) NRK cells at prophase (or early prometaphase) were injected with anti-p37 antibodies and fixed after they exited mitosis. Golgi membranes in the daughter cells were classified and counted. Means  $\pm$  SD (n = 8–9). An asterisk indicates a significant difference at  $p < 0.05$  compared with random IgG.

mock- and p37-depleted cells, indicating that p37 is not involved in ERAD.

### The p97/p37 Complex Shows Membrane Fusion Activity

To clarify the molecular function of p37 in Golgi biogenesis, we used an in vitro Golgi reassembly assay (Rabouille et al., 1995b). As shown in Figure 7A, anti-p37 antibodies partially inhibited cisternal regrowth caused by the addition of cytosol, which was enhanced by the addition of antibodies to p37 and p47 together. This result suggested a possible role for p37 in membrane fusion.

We tested this possibility by using purified proteins instead of cytosol; the results are shown in Figure 7B. There was little cisternal regrowth after incubation with either p97 or p37 alone. The p97/p37 complex, however, caused cisternal regrowth, and its fusion activity was increased by the addition of p115 to almost the same level as that of the p97/p47 complex. The cisternal regrowth caused by p97/p37 and p115 was inhibited by the addition of anti-p37 antibodies, but not by anti-p47 antibodies. Accordingly, the p97/p37 complex and p115 causes membrane fusion without the assistance of p47. Figure 7C shows the effect of varying the ratio of

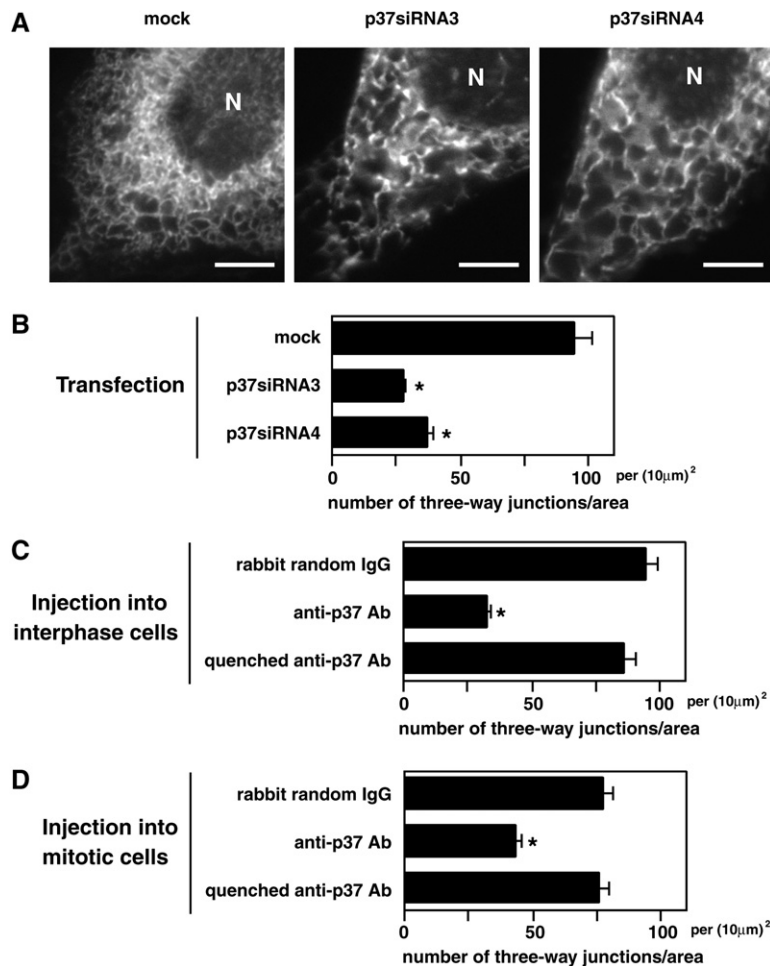


Figure 5. p37 Is Essential for the Biogenesis of the ER In Vivo

(A) CHO-K1 cells expressing GFP-tagged HSP47 were transfected with either mock or two distinct siRNA duplexes specific to p37. After incubation for 48 hr, ER structures were observed in living cells without fixation by confocal microscopy. Representative images of the ER after the transfection are shown. N; nucleus. The scale bar is 5  $\mu$ m.

(B) The numbers of ER three-way junctions in either mock- or p37 siRNA-treated cells were counted by using confocal microscopy as a parameter of ER network formation. Means  $\pm$  SD (n = 6–7). An asterisk indicates a significant difference at  $p < 0.05$  compared with mock (Bonferroni method).

(C) The cells at interphase were injected with anti-p37 antibodies and incubated for 4 hr. The cells that entered mitosis were removed every 1.5–2 hr during the incubation. After the incubation, the number of three-way junctions in ER network was counted. Means  $\pm$  SD (n = 7–8). An asterisk indicates a significant difference at  $p < 0.05$  compared with random IgG (control).

(D) The cells at prophase (or early prometaphase) were injected with anti-p37 antibodies. After they exited mitosis, the number of ER three-way junctions was counted. Means  $\pm$  SD (n = 8–9). An asterisk indicates a significant difference at  $p < 0.05$  compared with random IgG.

p37 to p97 on cisternal regrowth. Maximal regrowth occurred at 0.5 mol p37:1 mol p97, consistent with the proposed stoichiometry of the p97/p37 complex, namely, 2:1 (Figure 2C). It is likely that three molecules of p37 bind to a hexamer of p97.

It is reported that p115 binds to GM130 and functions as a tethering system in NSF-assisted Golgi reassembly (Nakamura et al., 1997). In contrast, the p97/p47 pathway does not require p115 (Rabouille et al., 1995a). We investigated, by using antibodies to p115 and GM130, whether p115 and GM130 are involved in p97/p37-dependent Golgi reassembly. As shown in Figure 7D, each antibody strongly inhibited p97/p37-dependent cisternal regrowth, but they had no effect on p97/p47-dependent regrowth. These results indicate that the p97/p37 pathway is distinct from the p97/p47 pathway requiring the presence of the p115-GM130 tethering system.

We next investigated whether VCIP135, an essential cofactor for p97/p47-assisted membrane fusion, is involved in the p97/p37 pathway (Figure 7E). Anti-VCIP135 antibodies inhibited cisternal regrowth caused by p97/p37, and the inhibition was rescued by quenching the antibodies with a VCIP135 fragment. These results suggest that VCIP135 is also involved in p97/p37-assisted membrane fusion events. Wang et al. (2004) have reported that VCIP135 shows deubiquitinating ac-

tivity and that p97/p47-dependent cisternal regrowth is inhibited by the addition of a ubiquitin mutant (Ile-44 to Ala, Ub[I44A]), which is unable to bind to p47. We therefore tested the effect of the ubiquitin mutant in the p97/p37 pathway (Figure 7F). The addition of Ub(I44A) during Golgi disassembly inhibited the cisternal regrowth caused by p97/p47, but it did not affect the regrowth caused by p97/p37.

The results of the Golgi reassembly assay with salt-washed mitotic Golgi fragments are presented in Figure 7G. When salt-washed membranes were incubated with p97/p37 and p115, no cisternal regrowth was observed. When VCIP135 together with p97/p37 and p115 were added, cisternal regrowth was observed. Thus, VCIP135 is an essential cofactor for p97/p37-dependent cisternal regrowth. Wang et al. (2004) also showed that neither VCIP135(C218S) nor VCIP135(C218A), which lack deubiquitinating activity, functioned in p97/p47-dependent Golgi reassembly. We tested these VCIP135 mutants in p97/p37-mediated activity (Figure 7G). There was no difference between VCIP135wt and mutants in p97/p37-dependent Golgi cisternal regrowth, although neither of the VCIP135 mutants functioned in p97/p47-dependent cisternal regrowth. These results clearly indicate that p97/p37-assisted membrane fusion requires VCIP135, but not its deubiquitinating activity.

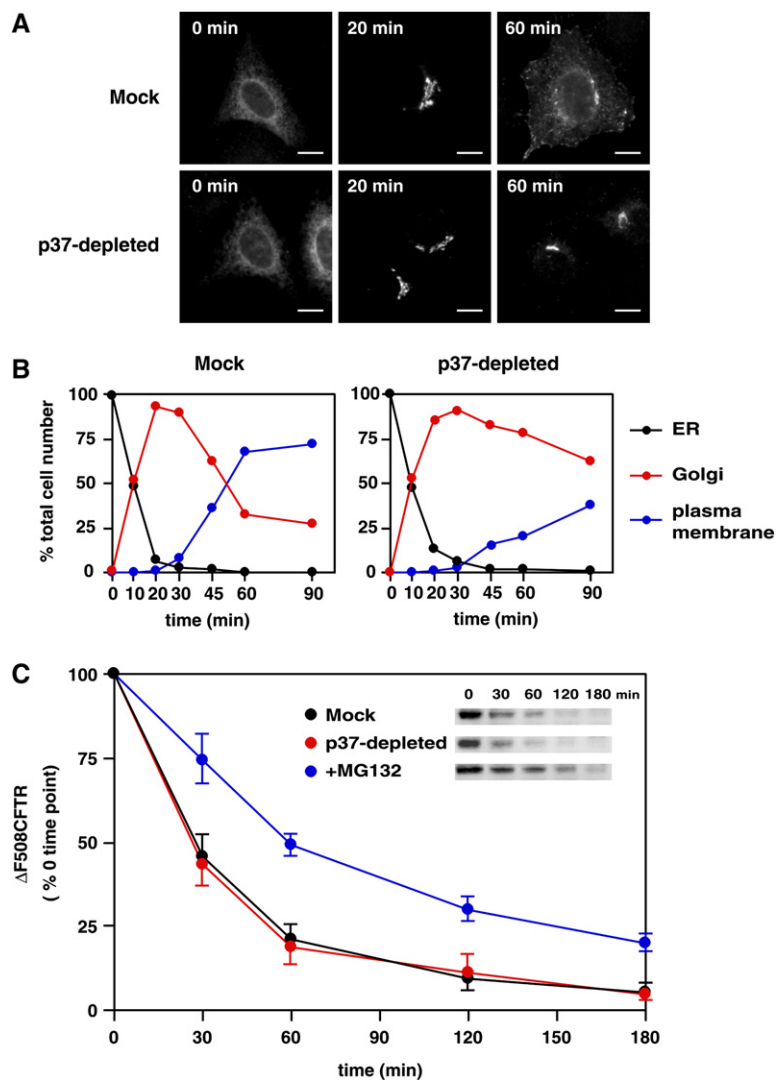


Figure 6. The Transport of VSV-G Is Delayed in p37-Depleted Cells

(A) Either mock-treated or p37 siRNA1-treated HeLa cells were transfected with ts045-VSV-G-GFP to measure the rate of membrane transport. ts045-VSV-G-GFP was stained with antibodies to GFP and observed by confocal microscopy. Representative images of cells for the 0, 20, and 60 min time points are shown to compare the transport of ts045-VSV-G-GFP in mock- and p37-depleted cells. The scale bar is 10  $\mu$ m.

(B) Three sets of cells were counted: one in which ts045-VSV-G-GFP remained at the ER network only; a second in which it was localized to the Golgi apparatus, but not to the plasma membrane; and a third in which it was transported to the plasma membranes. We counted 417–501 cells at each time point in either mock-treated or p37-depleted cells, and the percentages of cells in each set are shown.

(C) The effect of p37 on ERAD was clarified by investigating the turnover of  $\Delta$ F508CFTR in either mock- or p37 siRNA1-treated HeLa cells. As a positive control, MG132 (50  $\mu$ M, Calbiochem), a proteasome inhibitor, was added instead of siRNA treatment. The remaining amounts of  $\Delta$ F508CFTR in the cells were analyzed by western blotting with anti-CFTR monoclonal antibodies (insets). The western blotting results were quantified by using the NIH image, and the data for different time points were normalized relative to 100% for the 0 time point. Means  $\pm$  SD (n = 3).

### The p97/p37 Pathway Requires the SNARE GS15 in Golgi Reassembly

Muller et al. (2002) reported that NSF/SNAPs-dependent Golgi reassembly does not require the ATPase activity of NSF, since NSF/SNAPs has already dissociated the SNARE complexes during Golgi disassembly. To explore whether p97/p37 utilizes SNAREs primed by NSF/SNAPs during Golgi disassembly or whether it can dissociate SNARE complexes directly, we performed the *in vitro* Golgi disassembly in the presence of N-ethylmaleimide (NEM). In NEM-treated mitotic Golgi fragments, NEM inactivates endogenous NSF and prevents NSF/SNAPs-mediated SNARE dissociation. Using NSF-inactivated membranes, we tested the membrane fusion activity of p97/p37, as presented in Figure 8A. The untreated mitotic Golgi fragments were incubated with p97/NSF ATP-hydrolysis-deficient mutants (p97[E305Q,E578Q] or NSF[E329Q]), together with their respective cofactors. Cisternal regrowth was observed in NSF(E329Q)/SNAPs and p97wt/p37, but not in p97(E305Q,E578Q)/p37. When NEM-treated membranes were used, p97wt/p37 still caused cisternal regrowth, although NSF(E329Q)/SNAPs lost its membrane fusion activity. Hence, p97/p37 does

not utilize SNAREs primed by NSF/SNAPs during Golgi disassembly; i.e., the p97/p37 pathway dissociates SNARE complexes during Golgi reassembly without the assistance of NSF/SNAPs.

The p97/p47 pathway utilizes syntaxin5 as a SNARE (Rabouille et al., 1998). What SNAREs are involved in the p97/p37 pathway? As shown in Figure 8B, the addition of either anti-syntaxin5 antibodies or recombinant syntaxin5 lacking the transmembrane domain (a dominant-negative form of syntaxin5, syn5 $\Delta$ TM) had no effect on p97/p37-dependent cisternal regrowth, although both the antibodies and the dominant-negative syntaxin5 inhibited p97/p47-dependent cisternal regrowth. These results indicate that syntaxin5 is not involved in p97/p37-dependent Golgi reassembly. We next tested polyclonal antibodies raised against several known SNAREs (Gos28, Bet1, membrin, sec22b, GS15, and Ykt6), and we found that the addition of anti-GS15 antibodies inhibited p97/p37-dependent cisternal regrowth (Figure 8C). This inhibition was rescued by quenching the antibodies with a GS15 fragment. The addition of recombinant GS15 lacking the transmembrane domain (GS15 $\Delta$ TM) also showed a significant inhibitory effect.



These results strongly suggest that GS15 is involved in p97/p37-dependent Golgi reassembly.

In order to confirm these results biochemically, we performed immunoprecipitation experiments with p37-saturated Golgi membranes, as shown in Figures 8D and 8E. GS15 and p37 were coimmunoprecipitated, indicating that p37 is part of a GS15-containing complex.

Is the p97/p37/GS15-containing complex dissociated by p97-mediated ATP hydrolysis? We incubated salt-washed Golgi membranes together with His-p97 and His-p37. The isolated membranes were solubilized and used for immunoprecipitation with anti-GS15 antibodies and protein A beads. The beads were then incubated with VCIP135 in the presence of nucleotides. The results are presented in Figure 8F. The beads contained p97 and p37 (lane 1), which was consistent with the results shown in Figures 8D and 8E. When the beads were incubated together with VCIP135 in the presence of ATP, p97 and p37 were dissociated from the beads (lane 2). However, when the beads were incubated together with VCIP135 in the presence of AMP-PNP or ADP, p97 and p37 still remained on the beads (lanes 3 and 4). Upon incubation in the presence of ATP, but without VCIP135, the p97/p37/GS15-containing complex was not dissociated (lane 5). Considering that the p97/p37 pathway can prime SNAREs (see Figure 8A and its related text in Results), these results probably show that p97/p37 dissociates the SNARE complex by ATP hydrolysis with the assistance of VCIP135. VCIP135 bound to the beads in both the presence and the absence of p97 and p37 (lanes 1 and 6), and the amount remaining on the beads was slightly increased by incubation in the presence of AMP-PNP (lane 3).

The p97/p37/GS15-containing complex was also separated by SDS-PAGE, followed by silver staining. In addition to the bands of p97, p37, GS15, and immunoglobulin, we observed several bands of 20–35 kDa (data not shown), which might be other SNAREs or SNARE-like proteins involved in p97/p37-assisted fusion. We are now purifying the complex on a large scale for protein microsequencing.

## Discussion

In our previous work (Uchiyama et al., 2003), we reported that the p97/p47 pathway was less critical for Golgi maintenance during interphase compared to its reassembly at the end of mitosis. Since p97 localizes to the cytoplasm as well as the nucleus during interphase, we reasoned that p97 might have another adaptor protein for the maintenance of organelles in interphase. In this study, we searched for p97-binding proteins by yeast two-hybrid screening, and we have identified an adaptor protein, p37. p37 localizes to the cytoplasm as well as the nucleus, and it forms a complex with p97 in the cytosol. Our p37-knockdown experiments with siRNA revealed the important roles of p37 in the biogenesis of the Golgi and ER. Injection of anti-p37 antibodies into cells at different cell cycle stages also shows that p37 plays an important role in Golgi and ER maintenance during interphase as well as in their reassembly at the end of mitosis. In an *in vitro* Golgi reassembly assay, the p97/p37 complex displays membrane fusion activity. However, the p97/p37 pathway has a number of important

differences from the p97/p47 pathway (Table S1): (1) Unlike the p97/p47 pathway, the p97/p37 pathway requires p115 and GM130, a tethering protein and its binding partner, respectively. (2) p37 does not bind ubiquitin, while p47 binds monoubiquitin. (3) The p97/p37 pathway requires VCIP135, but not its deubiquitinating activity. (4) The p97/p37 pathway utilizes GS15 and other SNARE proteins, but not syntaxin5.

It has been reported that p115 and GM130 form a complex and function as a tethering system in the NSF-dependent membrane fusion pathway (Nakamura et al., 1997). Here, we also find that the p97/p37 pathway, unlike the p97/p47 pathway, requires the p115-GM130 tethering system. This specific requirement for a p115-GM130 tethering complex poses an interesting question regarding the control of the p97/p37 pathway during the cell cycle. Golgi disassembly-reassembly during mitosis requires the blocking of membrane fusion at early mitosis and its unblocking at late mitosis (Warren, 1993). At early mitosis, GM130 is phosphorylated, resulting in the disruption of the p115-GM130 tethering complex and subsequent mitotic inhibition of the NSF pathway (Lowe et al., 1998). The activity of NSF/SNAP-mediated SNARE priming is, however, maintained through mitosis (Muller et al., 2002). In the case of the p97/p47 pathway, p47 is also phosphorylated at early mitosis, which prevents the binding of p97/p47 to Golgi membranes and causes subsequent inhibition of p97/p47-assisted membrane fusion (Uchiyama et al., 2003). Thus, in contrast to the NSF pathway, the p97/p47-assisted fusion machinery *per se* is mitotically blocked.

This leads to the question as to how p97/p37-assisted membrane fusion is blocked during early mitosis. Considering that p97/p37 requires the p115-GM130 tethering complex, one possible explanation could be the disruption of the tethering complex by the mitotic phosphorylation of GM130, similar to the NSF pathway. However, several recent reports have raised concerns regarding the requirement for p115-GM130 tethering in trafficking. Vasile et al. (2003) have reported from the analysis of the temperature-sensitive conditional-lethal mutant *IdIG* that detectable levels (<5% of control) of GM130 were not always necessary for normal Golgi morphology. Linstedt and coworkers performed p115 siRNA knockdowns coupled with overexpression of a p115 mutant unable to bind GM130, and they observed that the p115 mutant could support normal Golgi structure (Puthenveedu and Linstedt, 2004). Shorter and Warren (1999) and our group (Uchiyama et al., 2003) showed that p97 was dissociated from mitotic Golgi membranes. Hence, it is likely that the p97/p37 complex is also dissociated from mitotic Golgi membranes in a manner similar to the p97/p47 complex, and that the p97/p37 fusion machinery *per se* is also mitotically blocked. Indeed, if the activity of p97/p37 is intact through mitosis, similar to what occurs with NSF/SNAPs, then SNAREs could be primed during Golgi disassembly, and the p97 hydrolysis mutant could then cause cisternal regrowth from NEM-untreated mitotic Golgi fragments. However, very little cisternal regrowth occurs with this p97 mutant (Figure 8A), supporting the notion that the activity of p97/p37 is inhibited during Golgi disassembly.

An important difference between p37 and p47 is the absence in p37 of a defined N-terminal UBA domain

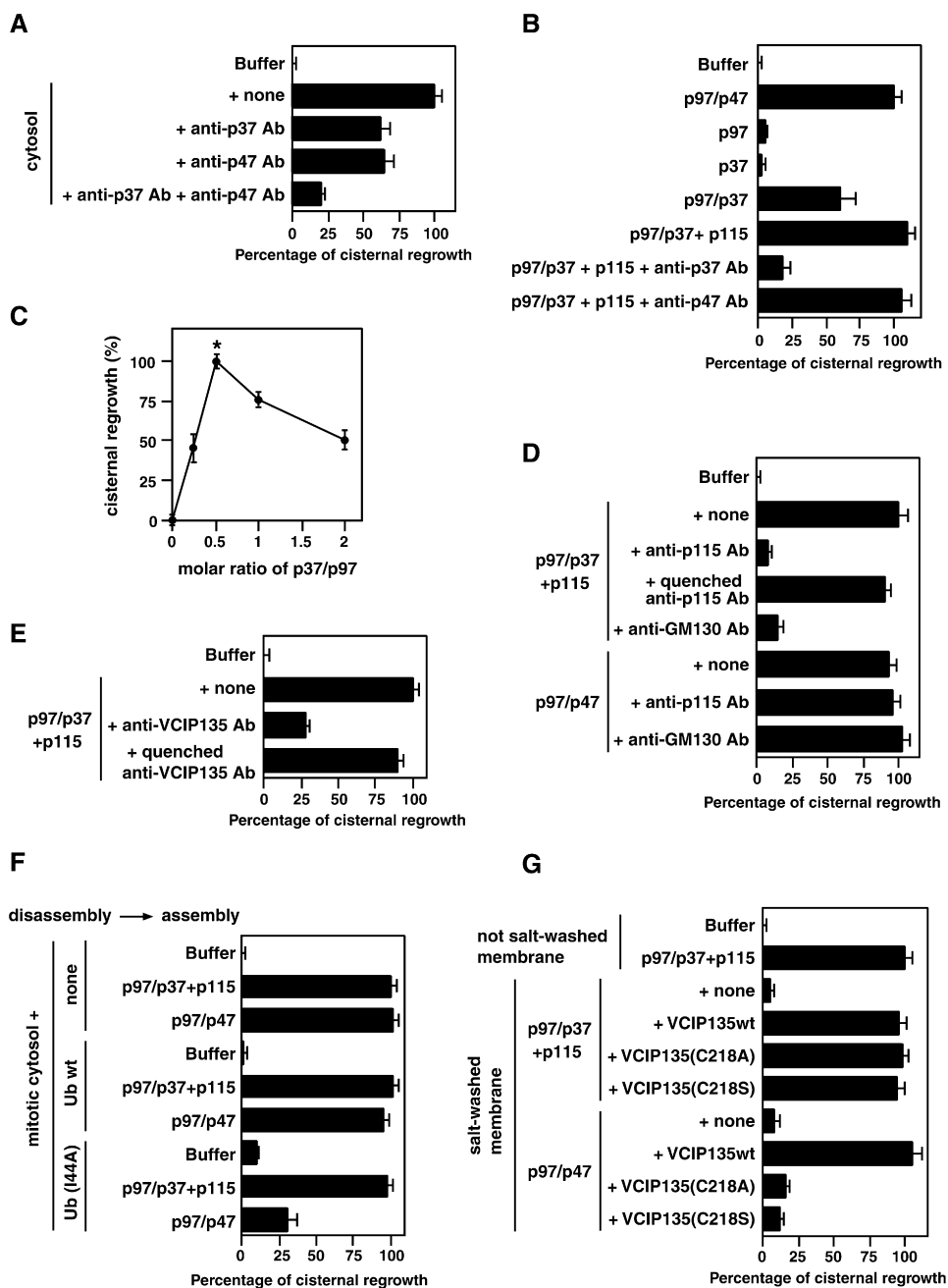


Figure 7. The p97/p37 Complex Shows Membrane Fusion Activity in an In Vitro Golgi Reassembly Assay

(A) Mitotic Golgi membranes were incubated with the indicated components at 37°C for 60 min. Cytosol (~10 mg/ml) was prepared from rat brain. Antibodies to p37 and p47 were polyclonal and affinity purified. The membranes were fixed and processed, and the percentage of membrane in cisterna was determined. Mean ± SD (n = 4); 0% represents the buffer (20.7% in cisternal membranes), and 100% represents the cytosol (44.8% in cisternal membranes).

(B) Mitotic Golgi membranes were incubated with the indicated components: p97 (50 μg/ml), p47 (20 μg/ml), p37 (19 μg/ml), p115 (30 μg/ml). Mean ± SD (n = 4); 0% represents the buffer (22.5% in cisternal membranes), and 100% represents p97/p47 alone (46.0% in cisternal membranes).

(C) p97 (50 μg/ml), p115 (30 μg/ml), and several doses of p37 (0, 4.8, 9.5, 19, 38 μg/ml) were incubated with mitotic membranes. Mean ± SD (n = 6); 0% represents p37/p97 = 0 (22.5% in cisternal membranes), and 100% represents p37/p97 = 0.5 (49.3% in cisternal membranes). An asterisk indicates a significant difference at p < 0.05 compared with the other points (Bonferroni method).

(D) Either anti-p115 or anti-GM130 antibodies were added to the indicated reassembly reactions as in (B). Mean ± SD (n = 4); 0% represents the buffer (23.2% in cisternal membranes), and 100% represents p97/p37 + p115 (49.1% in cisternal membranes).

(E) Anti-VCIP135 antibodies were added to mitotic Golgi membranes together with the p97/p37 complex and p115 as in (B). Mean ± SD (n = 4); 0% represents the buffer (24.8% in cisternal membranes), and 100% represents p97/p37 + p115 (48.5% in cisternal membranes).

(F) Golgi membranes were fragmented in the absence or presence of 40 μM exogenous ubiquitin (Ubwt) or the ubiquitin mutant (Ub[I44A]), followed by incubation with the indicated components as in (B). Mean ± SD (n = 4); 0% represents the buffer in the absence of exogenous Ub (26.2% in cisternal membranes), and 100% represents p97/p37 + p115 in the absence of exogenous Ub (51.2% in cisternal membranes).

(Figure 1A), which, in p47, has been shown to bind mono-ubiquitin, but not polyubiquitin, in the presence of p97 (Meyer et al., 2002). Furthermore, a p47 mutant lacking the UBA domain showed less membrane fusion activity in vitro (Meyer et al., 2002). The addition of a ubiquitin mutant (Ub[44A]) that cannot bind to p47 during Golgi disassembly inhibited p97/p47-dependent Golgi reassembly in vitro (Wang et al., 2004). VCIP135 mutants lacking deubiquitinating activity did not function in the p97/p47 pathway (Wang et al., 2004). Together, these results indicate that the p97/p47 pathway requires ubiquitylation-deubiquitination of as yet unknown factors. In contrast, no evidence was found to suggest the involvement of ubiquitin in the p97/p37 pathway. Our biochemical binding experiments reveal that p37 does not bind ubiquitin in either the absence or presence of p97 (Figure 2E). The addition of a ubiquitin mutant (I44A) during Golgi disassembly had no effect on p97/p37-dependent Golgi reassembly in vitro (Figure 7F). VCIP135 mutants (C218A and C218S) lacking deubiquitinating activity functioned in the p97/p37 pathway (Figure 7G). Considering these results, it is unlikely that the p97/p37 pathway requires ubiquitin for Golgi reassembly. What is the biological significance of the different requirement for ubiquitin in the two p97-mediated pathways? The p97/p47 pathway appears specialized for the reassembly of organelles at the end of mitosis (Uchiyama et al., 2003). Ubiquitylation is observed more widely during mitosis, and the requirement for ubiquitin in the p97/p47 pathway may contribute to its tight regulation during the cell cycle. Although a small amount of p47 is observed in the cytoplasm at interphase, it does not function in the maintenance of organelles (Uchiyama et al., 2003). A p47 mutant lacking its nuclear localization signals is microinjected into the cytoplasm of interphase cells to increase the amount of cytoplasmic p47, but we cannot observe any obvious morphological changes in the Golgi or ER (K.U. and H.K., unpublished data). These observations can be explained by the requirement for ubiquitin in the p97/p47 pathway.

VCIP135 is reported to act as a deubiquitinating enzyme in p97/p47-dependent Golgi reassembly (Wang et al., 2004), while it was originally identified as a p97/p47 complex-interacting protein (Uchiyama et al., 2002). In this study, we find that VCIP135 is required for the dissociation of the p97/p37/GS15-containing complex via p97-catalyzed ATP hydrolysis (Figure 8F, lanes 2 and 5). As p37 and p47 have very similar amino acid sequences, including their two p97 binding sites (Figure 1A), it is plausible that VCIP135 can also work as a p97/p37 complex-interacting protein and participate in the dissociation of the SNARE complex. These findings suggest that the function of VCIP135 in the priming of the SNARE complex is unlikely to require its deubiquitinating activity. VCIP135 therefore seems to work in two distinct ways: one via its deubiquitinating activity; the other in a ubiquitin-independent manner, perhaps as a p97/p37 (or p47) complex-interacting protein.

In our previous works and in this study, we have shown that p97 uses two distinct adaptors for its membrane fusion function: p47 is specialized for the reassembly of organelles at the end of mitosis; p37 is for organelle maintenance during interphase as well as for their reassembly during mitosis. Why are the two distinct p97 pathways required during the cell cycle? This leads to another question as to what mechanistic differences exist between the reassembly and maintenance of organelles. To answer these questions, much remains to be done to clarify the molecular mechanisms of the two p97 pathways.

## Experimental Procedures

### Proteins and Antibodies

p97, p47, Ufd1, Npl4, SVIP, syn5 $\Delta$ TM, p115, and Ub-GST were prepared as reported (Kondo et al., 1997; Meyer et al., 2000; Nagahama et al., 2003; Rabouille et al., 1995a, 1998; Wang et al., 2004). Polyclonal antibodies to p47, p97, VCIP135, and syntaxin5 were prepared as described (Kondo et al., 1997; Rabouille et al., 1998; Uchiyama et al., 2002, 2003), and polyclonal antibodies to GS15 and p115 were raised against His-GS15 $\Delta$ TM and His-p115(651–961). Monoclonal anti-PDI antibodies and polyclonal anti-GM130 antibodies were gifts from Dr. Vaux (Oxford University, UK) and Dr. Nakamura (Kanazawa University, Japan), respectively. Monoclonal antibodies to p97, His tag, GM130, mannosidase II, and CFTR were purchased from Progen, Qiagen, BD Transduction, Covance, and Upstate, respectively.

### Identification and cDNA Cloning of p37

The ORF of mouse p97 was subcloned into the yeast expression vector pGBKT7. The plasmid was transformed into yeast strain AH109, and a yeast two-hybrid screen was carried out essentially according to the manufacturer's protocol by using a GAL4 DNA activation domain fusion library in pACT2 (Mouse Brain MATCH-MAKER cDNA Library, Clontech). A total of  $1 \times 10^6$  colonies were screened, and 234 colonies were positive. One of them encoded p37, a protein similar to p47. Its full cDNA sequence (AK012822) was identified by an EST database search. The clone containing the full cDNA sequence of p37 was isolated from a mouse embryo cDNA library (Clontech) by PCR (primers: 5'-TGAGGGCCGCAAGCGGG-3', 5'-CAGAATAACAGGAAAACCAG-3'). This clone was sequenced, and a start codon was confirmed: it had a stop codon immediately upstream of the start codon. The ORF of p37 was subcloned into pQE30 by using BamHI and KpnI sites. Recombinant p37 was expressed in *E. coli* and was purified with Ni beads, followed by further purification with superdex 200 and mono Q columns (Pharmacia). His-tagged p37 was used to raise rabbit anti-p37 polyclonal antibodies. The resulting antibody was confirmed not to crossreact with p47.

### Biochemical Experiments

Competition experiments with GST-p97 and binding experiments with purified p97 and His-p37 were performed in buffer A (20 mM HEPEs, 1 mM MgCl<sub>2</sub>, 1 mM ATP, 1 mM DTT, 5% glycerol [pH 7.4]) containing 0.15 M KCl, 5 g/l trypsin inhibitor, and 0.1% Triton X-100. To clarify the distribution of p37, rat brain cytosol was fractionated by superose 6 (Pharmacia) in buffer A containing 0.15 M KCl. The binding experiments with Ub-GST were performed in buffer A containing 0.15 M KCl, 5 g/l trypsin inhibitor, and 0.5% Triton X-100.

For immunoprecipitation experiments with rat brain cytosol, the cytosol (70 mg total protein) was mixed with affinity-purified anti-p37 antibodies in buffer A containing 0.25 M KCl and 0.1% Triton X-100. p37 and its binding proteins were precipitated by proteinG beads.

(G) 1 M KCl-washed or unwashed mitotic Golgi membranes was incubated with several components or their combinations: p97 (50  $\mu$ g/ml), p47 (20  $\mu$ g/ml), p37 (19  $\mu$ g/ml), p115 (40  $\mu$ g/ml), VCIP135wt (18  $\mu$ g/ml), VCIP135(C218A) (18  $\mu$ g/ml), VCIP135(C218S) (18  $\mu$ g/ml). Mean  $\pm$  SD (n = 4); 0% represents the buffer (20.1% in cisternal membranes), and 100% represents non-salt-washed membranes with p97/p37 + p115 (49.0% in cisternal membranes).

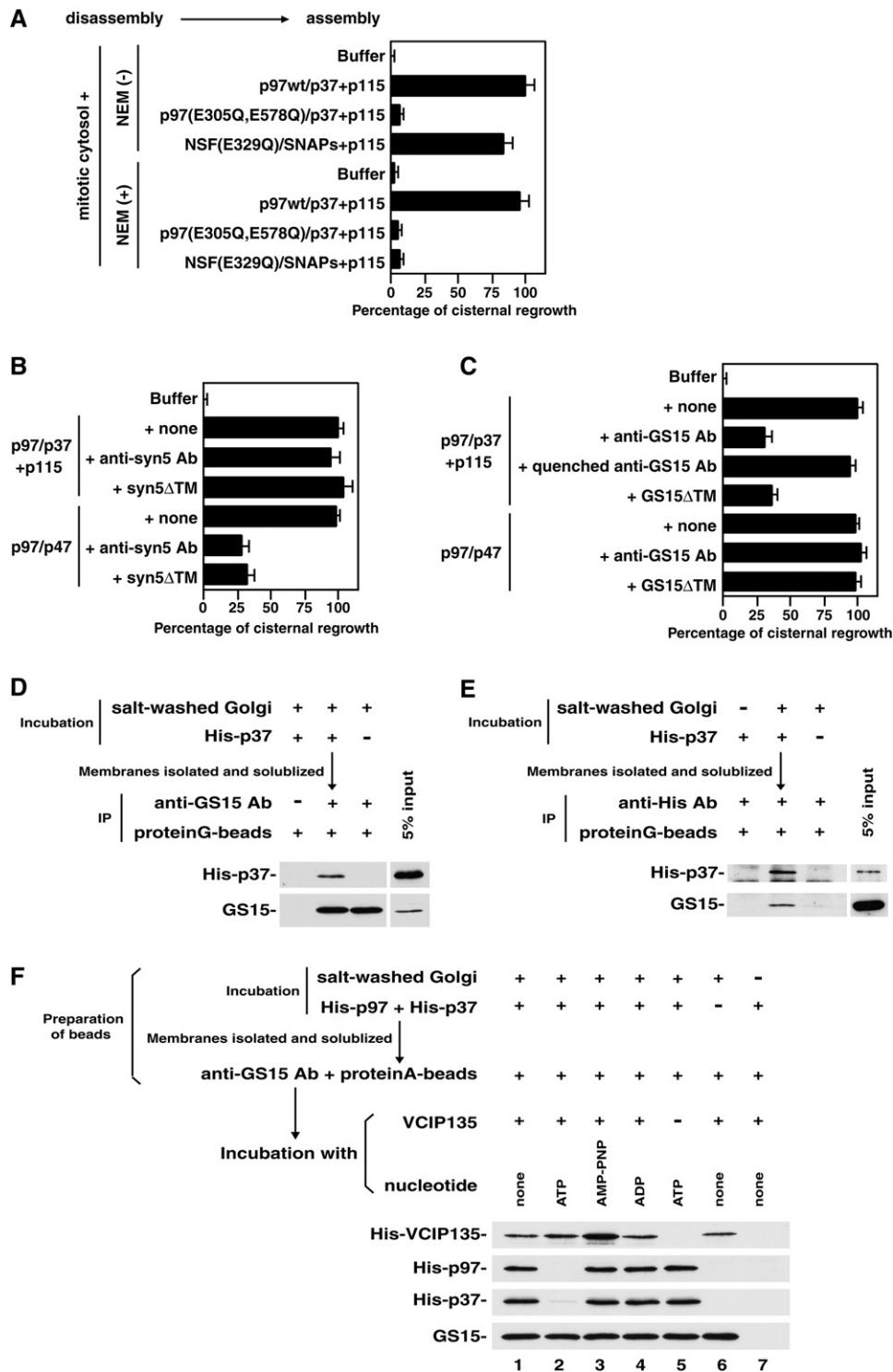


Figure 8. The p97/p37 Pathway Requires the SNARE GS15 in Golgi Reassembly

(A) Golgi membranes were fragmented in the absence or presence of 2.5 mM NEM, followed by incubation with the indicated components: p97 (50  $\mu$ g/ml), p97(E305Q,E578Q) (50  $\mu$ g/ml), p37 (19  $\mu$ g/ml), p115 (30  $\mu$ g/ml), NSF(E329Q) (100  $\mu$ g/ml),  $\alpha$ -SNAP (25  $\mu$ g/ml),  $\beta$ -SNAP (25  $\mu$ g/ml). Mean  $\pm$  SD (n = 4); 0% represents the buffer in the absence of NEM (23.8% in cisternal membranes), and 100% represents p97wt/p37 + p115 in the absence of NEM (49.7% in cisternal membranes).

(B) Either an anti-syntaxin5 antibody or syntaxin5 without TM (syn5 $\Delta$ TM, a dominant-negative form) was added to the indicated reassembly reactions: p97/p37 (50  $\mu$ g p97/ml), p97/p47 (50  $\mu$ g p97/ml), syn5 $\Delta$ TM (150  $\mu$ g/ml). Mean  $\pm$  SD (n = 4); 0% represents the buffer (25.7% in cisternal membranes), and 100% represents p97/p37 alone (52.0% in cisternal membranes).

(C) Either an anti-GS15 antibody or GS15 without TM (GS15 $\Delta$ TM, a dominant-negative form) was added to the indicated reassembly reactions: p97/p37 (50  $\mu$ g p97/ml), p97/p47 (50  $\mu$ g p97/ml), GS15 $\Delta$ TM (320  $\mu$ g/ml). Mean  $\pm$  SD (n = 4); 0% represents the buffer (23.4% in cisternal membranes), and 100% represents p97/p37 alone (49.8% in cisternal membranes).

For immunoprecipitation experiments with Golgi membranes, 1 M KCl-washed Golgi membranes (120  $\mu$ g) were first incubated with His-p37 (15  $\mu$ g) on ice for 1 hr. The isolated membranes were solubilized in 100  $\mu$ l buffer B (20 mM HEPES, 0.2 M KCl, 1 mM DTT, 1 mg/ml BSA [pH 7.4]) containing 10% glycerol and 2% CHAPS and were mixed with antibodies.

p97/p37/GS15-containing complexes were isolated and immobilized as follows. 1 M KCl-washed Golgi membranes (360  $\mu$ g) were incubated with His-p97 (40  $\mu$ g) and His-p37 (10  $\mu$ g). The isolated membranes were solubilized in 100  $\mu$ l buffer B containing 1 mM MgCl<sub>2</sub>, 10% glycerol, and 2% CHAPS and were mixed with anti-GS15 polyclonal antibodies (15  $\mu$ g) and protein G beads to prepare the beads of p97/p37/GS15-containing complexes. After washing with buffer B containing 1 mM MgCl<sub>2</sub>, 20% glycerol, and 0.1% Triton X-100, the beads were incubated together with His-VCIP135 (10  $\mu$ g) in the presence of the indicated nucleotides (10 mM) in a total volume of 200  $\mu$ l at 4°C for 3 hr.

#### Knockdown of p37 by siRNA

p37 was targeted with independent siRNAs (B-Bridge International): 5'-CAGUUUJAGAUGAUGGAGAA-3' (p37 siRNA1), 5'-CUCCAGAAGA GGAGGAUAA-3' (p37 siRNA2), 5'-ACUUGGAAGCCUUACACCU-3' (p37 siRNA3), 5'-CUUUUUUUUUGUGACUUA-3' (p37 siRNA4). p37 siRNA1 and p37 siRNA2 were used for HeLa cells, and p37 siRNA3 and p37 siRNA4 were used for CHO-K1 cells. Each 10 nM siRNA duplex was transfected by using lipofectamin RNAimax (Invitrogen), unless otherwise stated.

#### Injection of Antibodies and siRNA Duplexes into Cells

Either an affinity-purified antibody (~20 g/l) or random IgG (20 g/l) was injected together with the injection marker Cy3-BSA (~1 g/l). When injecting into interphase cells, the cells were incubated for 4 hr after the injection and were then fixed. The cells that entered mitosis were removed every 1.5–2 hr during the incubation in order to confirm that the remaining cells had never passed through mitosis. In the case of injection into mitotic cells, cells were roughly synchronized. Briefly, cells were cultured for 12 hr in the presence of aphidicolin (NRK cells, 0.5 mg/l; CHO-K1 cells, 0.25 mg/l). After washing out aphidicolin, they were cultured for an additional 4 hr and then injected.

The EM observation of injected cells was performed as described previously (Uchiyama et al., 2002, 2003). Cells were grown on a coverslip on which a square area of ~1 mm  $\times$  1 mm was outlined by a diamond pen. All cells within the area were injected and used for the EM observation.

For the EM study of siRNA-treated cells, each siRNA duplex (20  $\mu$ M) was injected three times at intervals of 24 hr into the cytoplasm of the cells within the area. Uninjected cells within the area were completely removed after every injection by an injection needle by using fluorescence of coinjected Cy3 as a marker. The cells were incubated for an additional 24 hr after the third injection and were then fixed.

For observation of ER structures, we used a stable CHO-K1 cell line expressing GFP-tagged HSP47, an ER protein (Uchiyama et al., 2002). ER structures were observed in living cells, without fixation, by using confocal microscopy.

#### VSV-G Transport Assay and $\Delta$ F508CFTR Degradation Assay

Each mock-treated or p37 siRNA-treated HeLa cell was transfected with ts045-VSV-G-GFP. The p37 siRNA1 duplex was used for the depletion of p37. Cells were first incubated for 2 hr at 37°C and then for 15 hr at 39.5°C. Before a temperature shift from 39.5°C to 32°C, cycloheximide (100  $\mu$ g/ml) was added to each dish, and cells were incubated at 4°C for 30 min. After 0, 10, 20, 30, 45, 60, and 90 min at 32°C, cells were fixed with paraformaldehyde, permeabilized with

Triton X-100, stained with monoclonal antibodies to GFP, and observed by confocal microscopy.

HeLa cells were transfected with a human  $\Delta$ F508CFTR expression vector (pFLAG-CMV-5A) 8 hr after mock or p37 siRNA treatment. p37 siRNA1 was used for the depletion of p37. Cells were incubated for 40 hr after transfection, and then cycloheximide (20  $\mu$ g/ml) was added into the culture medium. After incubation for the indicated time, cells were harvested and used to investigate  $\Delta$ F508CFTR turnover. To increase the expression level of  $\Delta$ F508CFTR, cells were incubated with 5 mM sodium butyrate for 16 hr before analysis.

#### In Vitro Golgi Reassembly Assay

The in vitro Golgi reassembly assay was performed as reported previously (Shorter and Warren, 1999). All proteins added in this assay were prepared as recombinant proteins from *E. coli*. The length of cisternae was measured by an intersection method (Rabouille et al., 1995b).

#### Supplemental Data

Supplemental Data include the depletion of p37 by p37 siRNA duplexes, the mapping of p37 for the binding to Golgi membranes, the interaction of p37 with SNAREs, and the comparison between the p97/p37 and p97/p47 pathways and are available at <http://www.developmentalcell.com/cgi/content/full/11/6/803/DC1/>.

#### Acknowledgments

We would like to thank C. Rabouille and N. Nakamura for their kind and helpful advice; M. Lindman for her kind assistance with the EM work; and S. Watanabe and H. Maekawa for their kind assistance with the yeast two-hybrid screening. We give special thanks to P. Luzio and the late K. Maruyama for their encouragement. M.P. is a student of the Vikki Graduate School in Bioscience. E.J. is funded by Helsinki University and the Academy of Finland. X.Z. and P.F. are funded by the Wellcome Trust. This work is supported by a grant to H.K. from the Ministry of Education, Culture, Sports, Science and Technology of Japan.

Received: June 30, 2005

Revised: September 8, 2006

Accepted: October 19, 2006

Published: December 4, 2006

#### References

- Dalal, S., Rosser, M.F., Cyr, D.M., and Hanson, P.I. (2004). Distinct roles for the AAA ATPases NSF and p97 in the secretory pathway. *Mol. Biol. Cell* 15, 637–648.
- Kondo, H., Rabouille, C., Newman, R., Levine, T.P., Pappin, D., Freemont, P., and Warren, G. (1997). p47 is a cofactor for p97-mediated membrane fusion. *Nature* 388, 75–78.
- Lowe, M., Rabouille, C., Nakamura, N., Watson, R., Jackman, M., Jamsa, E., Rahman, D., Pappin, D.J., and Warren, G. (1998). Cdc2 kinase directly phosphorylates the *cis*-Golgi matrix protein GM130 and is required for Golgi fragmentation in mitosis. *Cell* 94, 783–793.
- Lucocq, J.M., Berger, E.G., and Warren, G. (1989). Mitotic Golgi fragments in HeLa cells and their role in the reassembly pathway. *J. Cell Biol.* 109, 463–474.
- Meyer, H.H., Shorter, J.G., Seemann, J., Pappin, D., and Warren, G. (2000). A complex of mammalian ufd1 and npl4 links the AAA-ATPase, p97, to ubiquitin and nuclear transport pathways. *EMBO J.* 19, 2181–2192.

(D and E) Salt-washed Golgi membranes were first incubated in the presence of His-tagged p37. The isolated membranes were solubilized and mixed with either (D) anti-GS15 polyclonal or (E) anti-His monoclonal antibodies. The immunoprecipitates were fractionated by SDS-PAGE. The blots were probed with the following antibodies: anti-His monoclonal and anti-GS15 polyclonal antibodies in (D); anti-p37 and anti-GS15 polyclonal antibodies in (E).

(F) Salt-washed Golgi membranes were incubated with His-p97 and His-p37. The isolated membranes were solubilized and mixed with anti-GS15 antibodies and protein G beads. The resulting beads were incubated with or without His-VCIP135 in the presence of the indicated nucleotide. Proteins bound to the beads were fractionated by SDS-PAGE, followed by western blotting. The blots were probed with antibodies to p97, GS15, and His tag.

- Meyer, H.H., Wang, Y., and Warren, G. (2002). Direct binding of ubiquitin conjugates by the mammalian p97 adaptor complexes, p47 and Ufd1-Npl4. *EMBO J.* *21*, 5645–5652.
- Muller, J.M., Shorter, J., Newman, R., Deinhardt, K., Sagiv, Y., Elazar, Z., Warren, G., and Shima, D.T. (2002). Sequential SNARE disassembly and GATE-16-GOS-28 complex assembly mediated by distinct NSF activities drives Golgi membrane fusion. *J. Cell Biol.* *157*, 1161–1173.
- Nagahama, M., Suzuki, M., Hamada, Y., Hatsuzawa, K., Tani, K., Yamamoto, A., and Tagaya, M. (2003). SVIP is a novel VCP/p97-interacting protein whose expression causes cell vacuolation. *Mol. Biol. Cell* *14*, 262–273.
- Nakamura, N., Lowe, M., Levine, T.P., Rabouille, C., and Warren, G. (1997). The vesicle docking protein p115 binds GM130, a *cis*-Golgi matrix protein, in a mitotically regulated manner. *Cell* *89*, 445–455.
- Puthenveedu, M.A., and Linstedt, A.D. (2004). Gene replacement reveals that p115/SNARE interactions are essential for Golgi biogenesis. *Proc. Natl. Acad. Sci. USA* *101*, 1253–1256.
- Rabouille, C., Levine, T.P., Peters, J.M., and Warren, G. (1995a). An NSF-like ATPase, p97, and NSF mediate cisternal regrowth from mitotic Golgi fragments. *Cell* *82*, 905–914.
- Rabouille, C., Misteli, T., Watson, R., and Warren, G. (1995b). Reassembly of Golgi stacks from mitotic Golgi fragments in a cell-free system. *J. Cell Biol.* *129*, 605–618.
- Rabouille, C., Kondo, H., Newman, R., Hui, N., Freemont, P., and Warren, G. (1998). Syntaxin 5 is a common component of the NSF- and p97-mediated reassembly pathways of Golgi cisternae from mitotic Golgi fragments in vitro. *Cell* *92*, 603–610.
- Shorter, J., and Warren, G. (1999). A role for the vesicle tethering protein, p115, in the post-mitotic stacking of reassembling Golgi cisternae in a cell-free system. *J. Cell Biol.* *146*, 57–70.
- Uchiyama, K., Jokitalo, E., Kano, F., Murata, M., Zhang, X., Canas, B., Newman, R., Rabouille, C., Pappin, D., Freemont, P., and Kondo, H. (2002). VCIP135, a novel essential factor for p97/p47-mediated membrane fusion, is required for Golgi and ER assembly in vivo. *J. Cell Biol.* *159*, 855–866.
- Uchiyama, K., Jokitalo, E., Lindman, M., Jackman, M., Kano, F., Murata, M., Zhang, X., and Kondo, H. (2003). The localization and phosphorylation of p47 are important for Golgi disassembly-assembly during the cell cycle. *J. Cell Biol.* *161*, 1067–1079.
- Vasile, E., Perez, T., Nakamura, N., and Krieger, M. (2003). Structural integrity of the Golgi is temperature sensitive in conditional-lethal mutants with no detectable GM130. *Traffic* *4*, 254–272.
- Wang, Y., Satoh, A., Warren, G., and Meyer, H.H. (2004). VCIP135 acts as a deubiquitinating enzyme during p97-p47-mediated reassembly of mitotic Golgi fragments. *J. Cell Biol.* *164*, 973–978.
- Warren, G. (1993). Membrane partitioning during cell division. *Annu. Rev. Biochem.* *62*, 323–348.
- Ye, Y., Meyer, H.H., and Rapoport, T.A. (2001). The AAA ATPase Cdc48/p97 and its partners transport proteins from the ER into the cytosol. *Nature* *414*, 652–656.

#### Accession Numbers

The p37 nucleotide sequence is available in the DNA Data Bank of Japan database under accession code [AB120715](#).